ISET Journal of Earthquake Technology, Paper No. 442, Vol. 41, No. 1, March 2004, pp. 101-125

STORY SHEAR STRENGTH PATTERNS FOR THE PERFORMANCE-BASED SEISMIC DESIGN OF REGULAR FRAMES

Ricardo A. Medina
Department of Civil and Environmental Engineering
University of Maryland
College Park, MD 20742, U.S.A.

ABSTRACT

This study investigates the dependence of the magnitude and the distribution of story ductility demands over the height of regular frames on the design story shear strength distribution. Regular frames subjected to ordinary ground motions with story shear strength distributions based on parabolic, triangular, and uniform design load patterns are studied. Results from this work suggest that for non-deteriorating, regular frames, the parabolic load pattern is more effective to limit the story ductility demands at the top of the structure, while the triangular and uniform load patterns are more effective to limit the story ductility demands at the bottom stories. Design story shear strength patterns are proposed based on the premise that an optimum design lateral load pattern would result in a uniform distribution of story ductilities over the height. The proposed design story shear strength patterns are a function of the ground motion and structural characteristics, as well as the performance level of interest, and they are deemed to be useful for the preliminary design of frame structures.

KEYWORDS: Story Ductility, Deformation Demands, Building Frames, Design Story Shear Strength, Performance-Based Design

INTRODUCTION

Current seismic design criteria in the United States are based on story shear strength patterns developed from well-established dynamic analysis concepts (ATC, 1978; FEMA, 2000a; IBC, 2003). These shear strength patterns represent the expected distribution of the maximum inertia forces that a system experiences when it is subjected to seismic excitations. The shape of the code-compliant shear strength distributions takes into account the most important dynamic characteristics that influence the behavior of multi-story buildings (e.g., higher mode effects). Frame structures subjected to strong ground shaking are generally designed with sufficient deformation capacity to undergo significant levels of inelastic behavior. However, the inelastic dynamic behavior of structures is not very well understood, and the designer has limited control over the extent of damage that a system will experience and its distribution in the structure. Results from this study suggest that in some cases, designing frames using story shear strength patterns based on elastic dynamic analysis concepts may not be the best alternative to mitigate the occurrence and/or the extent of damage in frames that experience considerable levels of inelastic deformation. The problem becomes more complex when issues such as the P-Delta effects, structure overstrength, cyclic deterioration and the contribution of nonstructural components to the response are present.

The main objectives of this study are to (a) provide additional insight into the inelastic dynamic behavior of frames whose strength design is based on various pre-defined lateral load patterns, and (b) recommend design story shear strength patterns to control the extent of damage in multi-story frames exposed to ordinary ground motions. In this context, damage control is a function of the performance target of interest and implies a design in which the amount of damage is limited, and it is uniformly distributed over the height of the frame. Therefore, the energy dissipation capacity of all structural elements can be efficiently utilized. Issues such as structure P-Delta are considered; however, cyclic deterioration, overstrength and the contribution of nonstructural components to the response are not investigated. Therefore, the inelastic deformation levels of primary interest are those that correspond to demands at which significant cyclic deterioration is not expected to occur (displacement ductility less than about 6).

In this paper, the term 'damage' refers to structural damage to frame structures when no additional energy dissipation mechanisms are included (e.g., active or passive control strategies). The basic engineering demand parameter used to quantify structural damage is the story ductility, which is defined as the ratio of the maximum story drift from a time history analysis to the story yield drift from a pushover analysis based on a predetermined lateral load distribution. A parametric study is performed in which the statistical quantification of results is carried out to account for the inherent randomness in ground motion characteristics.

This research provides comprehensive information on static story shear strength patterns that are useful in the conceptual design of frames subjected to ground motion hazards characteristic of ordinary ground motions.

Table 1: LMSR-N Ground Motion Set

Record ID	Event	Year	Moment Magnitude	Station	Closest Distance (km)
IV79cal	Imperial Valley	1979	6.5	Calipatria Fire Station	23.8
IV79chi	Imperial Valley	1979	6.5	Chihuahua	28.7
IV79cmp	Imperial Valley	1979	6.5	Compuertas	32.6
IV79e01	Imperial Valley	1979	6.5	El Centro Array #1	15.5
IV79e12	Imperial Valley	1979	6.5	El Centro Array #12	18.2
IV79e13	Imperial Valley	1979	6.5	El Centro Array #13	21.9
IV79nil	Imperial Valley	1979	6.5	Niland Fire Station	35.9
IV79pls	Imperial Valley	1979	6.5	Plaster City	31.7
IV79qkp	Imperial Valley	1979	6.5	Cucapah	23.6
IV79wsm	Imperial Valley	1979	6.5	Westmorland Fire Station	15.1
LP89agw	Loma Prieta	1989	6.9	Agnews State Hospital	28.2
LP89cap	Loma Prieta	1989	6.9	Capitola	14.5
LP89g03	Loma Prieta	1989	6.9	Gilroy Array #3	14.4
LP89g04	Loma Prieta	1989	6.9	Gilroy Array #4	16.1
LP89gmr	Loma Prieta	1989	6.9	Gilroy Array #7	24.2
LP89hch	Loma Prieta	1989	6.9	Hollister City Hall	28.2
LP89hda	Loma Prieta	1989	6.9	Hollister Differential Array	25.8
LP89hvr	Loma Prieta	1989	6.9	Halls Valley	31.6
LP89sjw	Loma Prieta	1989	6.9	Salinas - John & Work	32.6
LP89slc	Loma Prieta	1989	6.9	Palo Alto - SLAC Lab.	36.3
LP89svl	Loma Prieta	1989	6.9	Sunnyvale - Colton Ave.	28.8
NR94cen	Northridge	1994	6.7	LA - Centinela St.	30.9
NR94cnp	Northridge	1994	6.7	Canoga Park - Topanga Can.	15.8
NR94far	Northridge	1994	6.7	LA - N Faring Rd.	23.9
NR94fle	Northridge	1994	6.7	LA - Fletcher Dr.	29.5
NR94glp	Northridge	1994	6.7	Glendale - Las Palmas	25.4
NR94hol	Northridge	1994	6.7	LA - Holywood Stor FF	25.5
NR94lh1	Northridge	1994	6.7	Lake Hughes #1 #	36.3
NR94lv2	Northridge	1994	6.7	Leona Valley #2 #	37.7
NR94lv6	Northridge	1994	6.7	Leona Valley #6	38.5
NR94nya	Northridge	1994	6.7	La Crescenta-New York	22.3
NR94pic	Northridge	1994	6.7	LA - Pico & Sentous	32.7
NR94stc	Northridge	1994	6.7	Northridge - 17645 Saticoy St	13.3
NR94stn	Northridge	1994	6.7	LA - Saturn St	30.0
NR94ver	Northridge	1994	6.7	LA - E Vernon Ave	39.3
SF71pel	San Fernando	1971	6.6	LA - Hollywood Stor Lot	21.2
SH87bra	Superstition Hills	1987	6.7	Brawley	18.2
SH87icc	Superstition Hills	1987	6.7	El Centro Imp. Co. Cent	13.9
SH87pls	Superstition Hills	1987	6.7	Plaster City	21.0
SH87wsm	Superstition Hills	1987	6.7	Westmorland Fire Station	13.3

GROUND MOTIONS USED IN THIS STUDY

A set of 40 ordinary ground motions (denoted as LMSR-N set) is used to carry out the seismic demand evaluation of non-deteriorating regular frames. Ordinary ground motions are those that do not exhibit (a) near-fault, forward directivity; (b) soft soil or (c) long duration characteristics. Californian earthquakes of moment magnitude between 6.5 and 6.9 and closest distance to the fault rupture between 13 km and 40 km are studied (Table 1). These ground motions are recorded on soils that correspond to NEHRP site class D (FEMA, 2000a). The records are selected from the PEER (Pacific Earthquake Engineering Research) Center Ground Motion Database (http://peer.berkeley.edu/smcat/). A

comprehensive documentation of the properties of the LMSR-N ground motion set is presented in Medina and Krawinkler (2003).

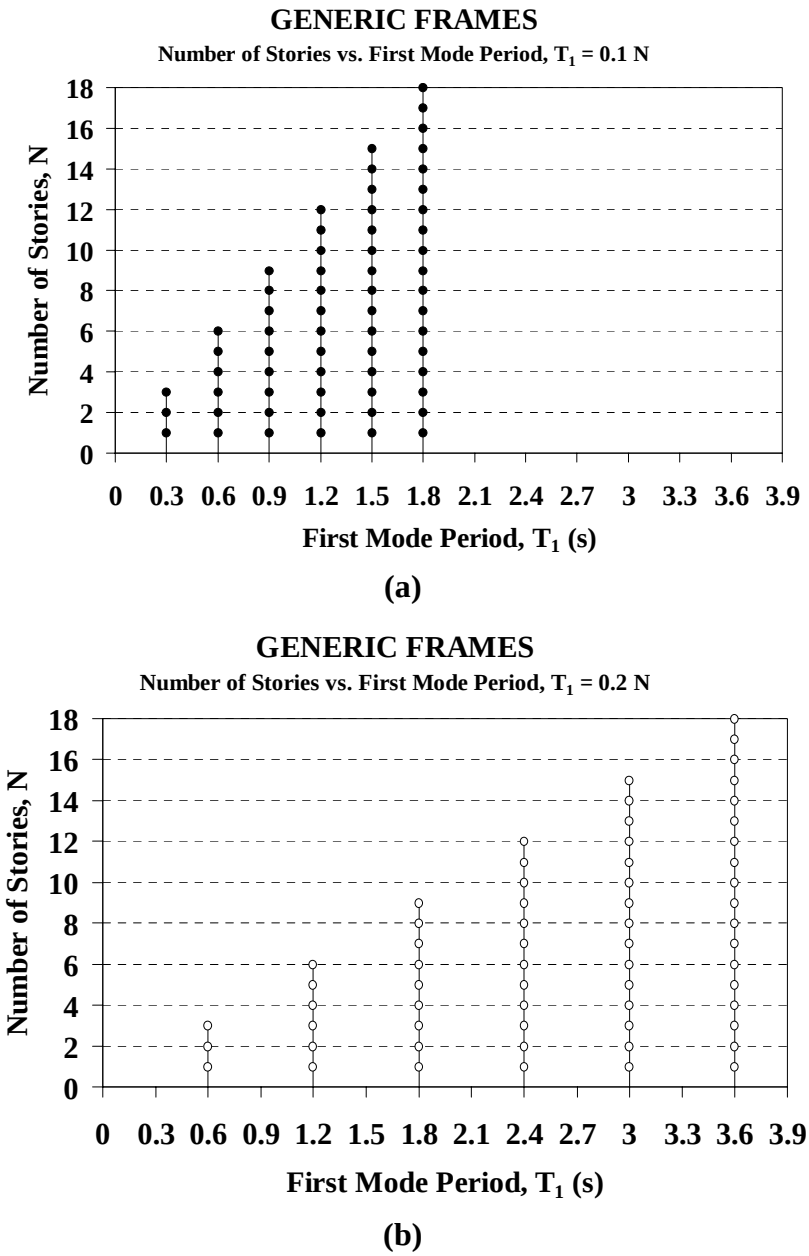

Fig. 1 Single-bay, generic frames: (a) stiff and (b) flexible

STRUCTURAL MODELS

Single-bay, generic frame models with number of stories, N, equal to 3, 6, 9, 12, 15, and 18, and fundamental periods, T_1, of $0.1N$ and $0.2N$ are used (see Figure 1). The overlaps at T_1 = 0.6 s, 1.2 s and 1.8 s allow an assessment of the effect of the number of stories (or global stiffness) in the response of the frames given T_1. The criterion, $T_1 = 0.1N$ or $0.2N$, also provides the basis to assign absolute values of stiffness to the various members of the structure. Results obtained by Medina and Krawinkler (2003) demonstrate that single-bay generic frame models are adequate to represent the global dynamic behavior of more complex regular multi-story frames exposed to earthquake excitations.

The main characteristics of the family of structures used in this study are as follows:

- Models are two-dimensional.
- The same mass is used at all floor levels.

- Frames have a single bay and a constant story height equal to 3.66 m (12 feet) and a beam span equal to 7.32 m (24 feet).
- Centerline dimensions are used for beam and column elements (i.e., the effect of finite joint regions is neglected).
- Each story stiffness is tuned so that when the frame is subjected to a triangular load pattern there is a uniform distribution of story drifts over the height. This criterion translates into a straight-line first mode for all frames, which in turns provides the distribution of relative member stiffnesses along the height.
- Frames are designed based on the strong column-weak girder philosophy that is, plastification is only allowed to occur at the end of beams and the bottom of the first story columns (see Figure 2(a)).
- Member, and hence, story strengths are tuned so that simultaneous yielding along the height is attained under a pre-defined load pattern.
- The moment-rotation hysteretic behavior is modeled by using rotational springs with peak-oriented hysteretic rules and 3% strain hardening (see Figure 2(b)).
- Global (structure) P-Delta is included (member P-Delta is ignored). P-Delta effects are quantified by the elastic first story stability coefficient, θ, which is defined as $\theta = P\delta_{s1} / V_1 h_1$, where P is the axial load in the first story columns, δ_{s1} and V_1 are the first story drift and shear force, respectively, and h_1 is the first story height. P is the dead load plus a live load equal to 40% of the dead load. Values for the elastic first story stability coefficient of the models used in this study are shown in Figure 3.

For the time-history analyses, 5% Rayleigh damping is assigned to the first mode and the mode at which the cumulative mass participation exceeds 95%.

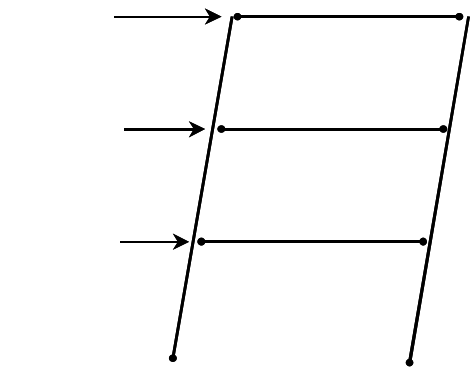

(a)

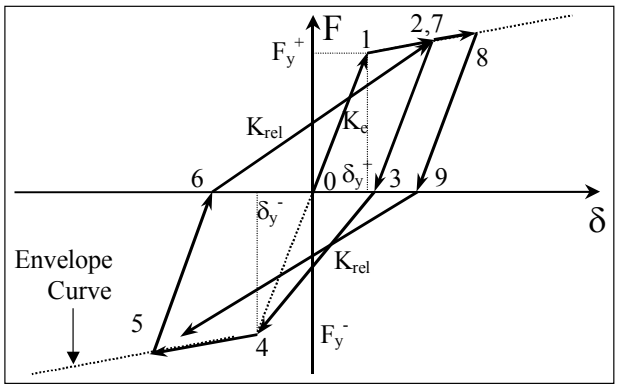

(b)

Fig. 2 (a) Beam-hinge mechanism and (b) Peak-oriented hysteretic behavior

EFFECT OF DESIGN STORY SHEAR STRENGTH PATTERNS ON STORY DUCTILITY DEMANDS

It is postulated that story ductility demands are relevant engineering demand parameters to quantify structural damage in frame structures. However, it is important to recognize that any definition of story

ductility is a function of the story yield drift, which is not a well defined quantity in most cases. Simplified approaches are available to estimate story yield drifts (ATC, 1996; FEMA, 2000b), but in this study, the story yield drift is a well defined quantity, since frames are designed so that simultaneous yielding occurs in all stories under a pre-defined load pattern. This work focuses on the sensitivity of story ductility demands to various strength distributions with the stiffness distribution remaining constant.

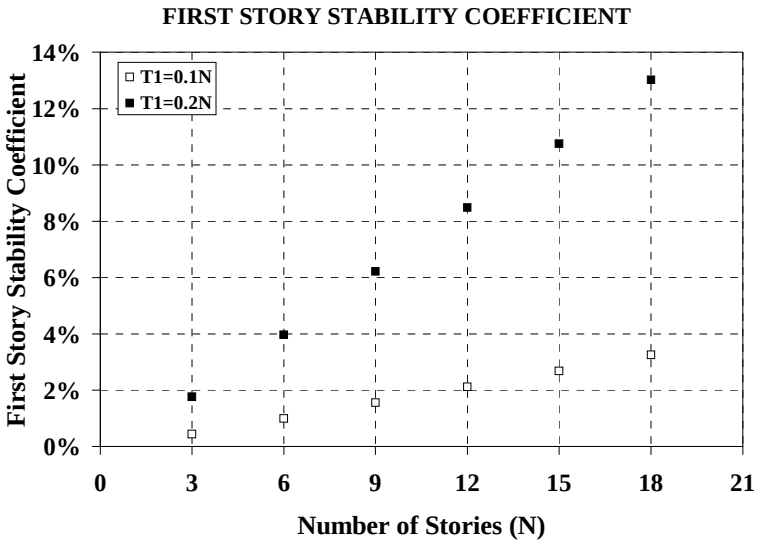

Fig. 3 Elastic first story stability coefficient for the family of single-bay, generic frames

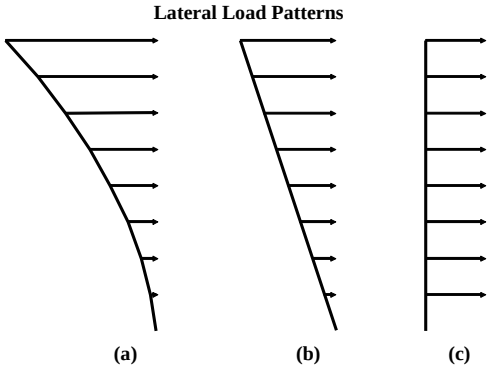

Fig. 4 Design lateral load patterns: (a) parabolic, (b) triangular and (c) uniform

Extensive time history analyses are performed for all frames and the LMSR-N set of ground motions using the DRAIN-2DX computer program (Prakash et al., 1993). Three basic design story shear strength patterns are used. These patterns are derived from parabolic, triangular and uniform loading (Figure 4). For regular buildings that is, structures without significant mass or stiffness irregularities, story strength distributions based on parabolic and triangular load patterns correspond to those recommended by NEHRP (FEMA, 2000a) for k values equal to 2 and 1, respectively (see Equations (1) and (2)). A story shear strength distribution, based on a uniform load pattern, corresponds to $k = 0$ in Equation (2).

$$F_x = C_{vx} V \tag{1}$$

and

$$C_{vx} = \frac{w_x h_x^k}{\sum_{i=1}^{n} w_i h_i^k} \tag{2}$$

where F_x is the lateral load at level x, C_{vx} is the vertical distribution factor, V is the total design lateral force or shear at the base of the structure, w_i and w_x are the portion of the total seismic effective weight of the structure, W, located or assigned to level i or x, h_i and h_x are the height from the base to level i or x, and k is an exponent related to the structure period.

1. Graphical Representation of Results

The control parameter used to relate the ground motion intensity with the structure strength is the parameter $[S_a(T_1)/g]/\gamma$, where $S_a(T_1)$ is the 5% damped spectral acceleration at the fundamental period of the structure, and γ is base shear coefficient that is, $\gamma = V_y/W$, with V_y being the yield base shear strength. The parameter $[S_a(T_1)/g]/\gamma$ represents the ductility-dependent response modification factor (often denoted as R_μ), which in the context of present codes is equal to the conventional R-factor if no overstrength is present (if it is necessary, the effect of overstrength could be taken into account by modifying the denominator of the parameter $[S_a(T_1)/g]/\gamma$).

The basic graphical communication scheme from which results are derived is presented in Figure 5 for the N = 9, T_1 = 0.9 s frame, a relative intensity $[S_a(T_1)/g]/\gamma$ = 4.0 and the LMSR-N set of ground motions. Figure 5 shows the relative height plotted on the vertical axis and the story ductility plotted on the horizontal axis. In this representation, a vertical line implies a uniform distribution of story ductilities over the height. The gray lines correspond to the responses to the individual records. The median is defined as the average between the 20th and 21st sorted values, the average between the 6th and 7th sorted values is the 16th percentile, and the 84th percentile is the average between the 33rd and 34th sorted values.

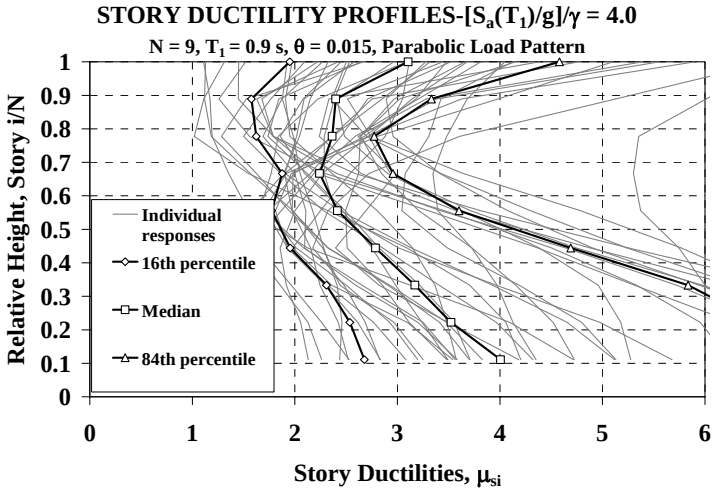

Fig. 5 Distribution of story ductilities over the height, N = 9, T_1 = 0.9 s, $[S_a(T_1)/g]/\gamma$ = 4.0, LMSR-N set of ground motions

2. Sensitivity of Story Ductility Demands to the Design Story Shear Strength Pattern

Representative results from time-history analyses are shown for the 3, 9 and 18 story frames with $T_1 = 0.1N$ and $0.2N$. Figures 6 to 9 present median values for the distribution of story ductility demands over the height of frames for a given relative intensity ($[S_a(T_1)/g]/\gamma$). As expected, median story ductility demands tend to increase with an increase in the relative intensity. Moreover, the distribution and magnitude of story ductilities over the height are highly dependent on the design load pattern. In some cases (e.g., Figures 8 and 9), no median value is reported for the N = 18, T_1 = 3.6 s frame because at these relative intensities, more than 50% of the records have caused global collapse of the system due to second order, P-Delta effects.

In general, for all relative intensities, structures designed based on a parabolic load pattern experience smaller median story ductility demands at the top of the structure while structures designed based on a uniform load pattern present smaller story ductility demands at the bottom stories. A design based on a triangular load pattern yields median story ductility values that are in between those obtained from the parabolic and uniform load patterns. Even for relatively strong structures, $[S_a(T_1)/g]/\gamma$ = 1.0, early yielding occurs at the top stories, especially for the long period systems $T_1 \geq 1.8$ s, regardless of the design story shear strength pattern. This behavior is consistent with the fact that the story strength distribution of the generic frames is tuned to a pre-defined lateral load pattern; thus, upper stories are designed for a smaller strength than the one required for the design of real buildings, in which gravity loads tend to control the beam strength in the upper stories. Thus, the effect of tuning the structure strength to a design load pattern produces "weak" upper stories and a dynamic response in which yielding may occur along the height of the frame, with the largest level of inelastic behavior occurring at the top of

the structure. This phenomenon is illustrated in Figure 10 for the $N = 9$, $T_1 = 1.8$ s frame with a base shear coefficient, $\gamma = 0.18$, which in this case corresponds to $[S_a(T_1)/g]/\gamma = 2.0$, since all records are scaled to $S_a(1.8\text{ s}) = 0.36g$.

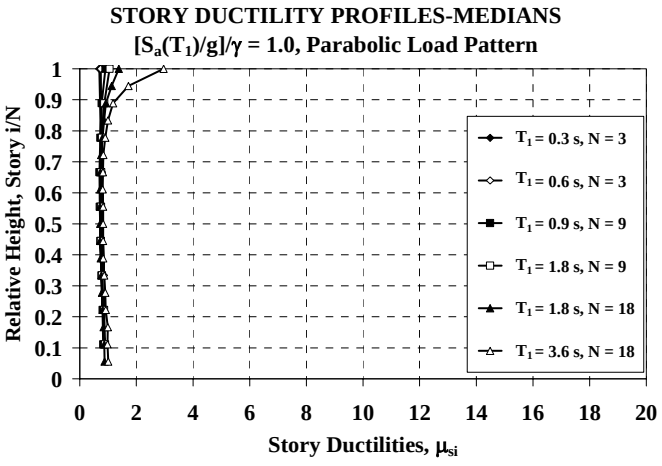

(a)

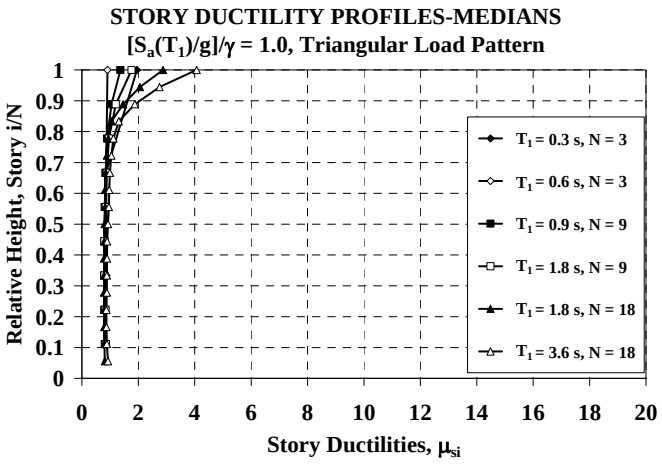

(b)

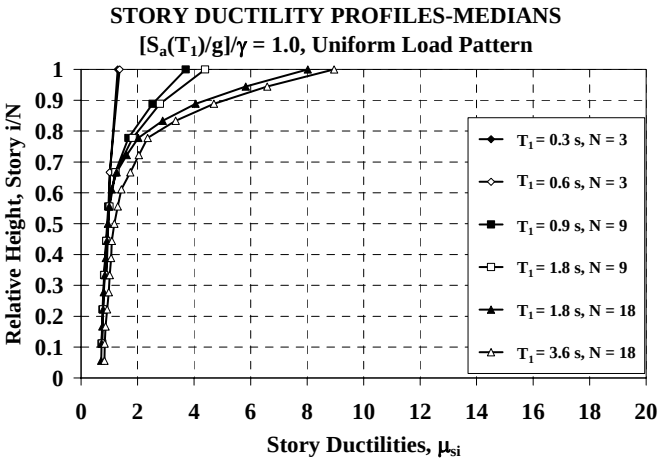

(c)

Fig. 6 Median story ductility profiles, N = 3, 9 and 18, T_1 = 0.1N and 0.2N, $[S_a(T_1)/g]/\gamma$ = 1.0, various design load patterns: (a) parabolic, (b) triangular, and (c) uniform

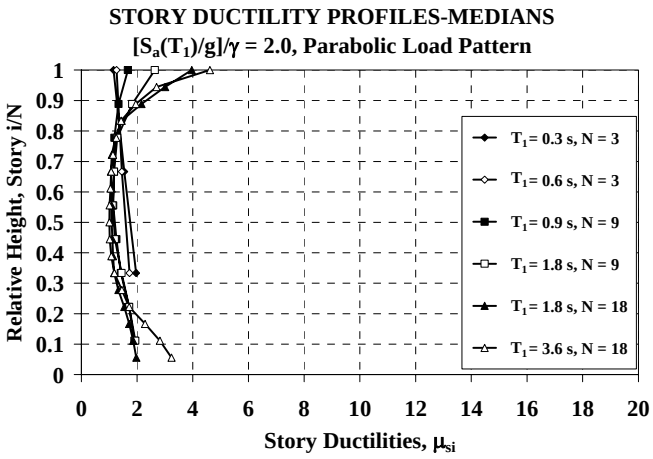

(a)

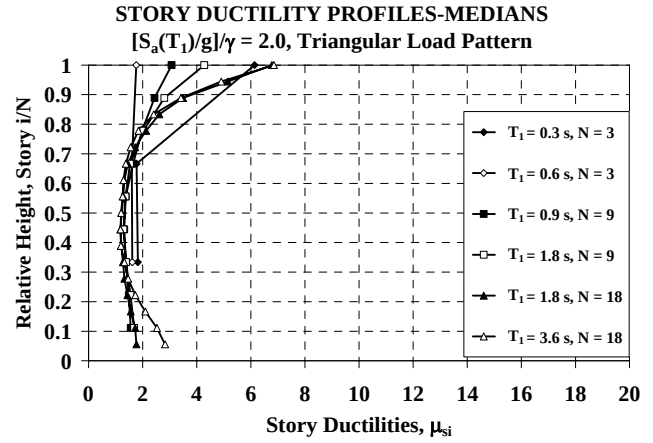

(b)

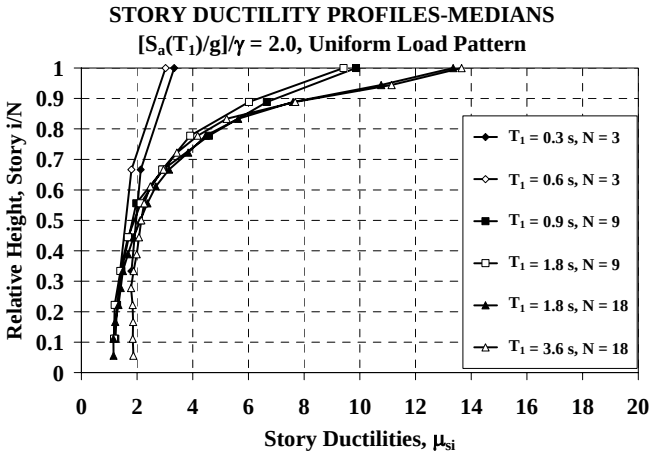

(c)

Fig. 7 Median story ductility profiles, N = 3, 9 and 18, T_1 = 0.1N and 0.2N, $[S_a(T_1)/g]/\gamma$ = 2.0, various design load patterns: (a) parabolic, (b) triangular, and (c) uniform

The main conclusion is that for ordinary ground motions, the distribution of structural damage over the height of a frame is sensitive to the design story shear strength pattern and the level of inelastic behavior in a system.

Results obtained in this research are based on frame models that exhibit peak-oriented hysteretic behavior at plastic hinge locations. Medina and Krawinkler (2003) evaluate the effect of different hysteretic models (bilinear, peak-oriented and pinching) on the displacement response of the family of generic frame models. The general conclusion is that the "pinched" model (severe pinching of hysteresis

loops) leads to somewhat greater story ductility (and drift) demands than the peak oriented and bilinear models, while the latter two exhibit similar deformation demands. However, this pattern is reversed in the case of flexible structures that are P-Delta sensitive. In this case, the bilinear model predicts the largest story drift demands because it spends the most time on the backbone of the response curve, which for P-Delta sensitive structures has a negative post-yield tangent stiffness that leads to "ratcheting" of the response.

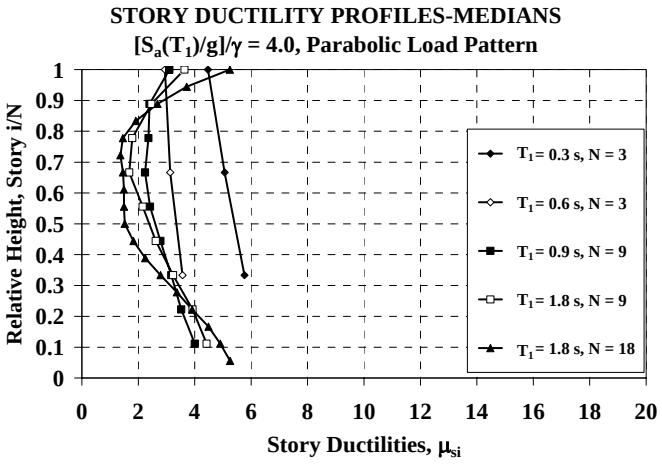

(a)

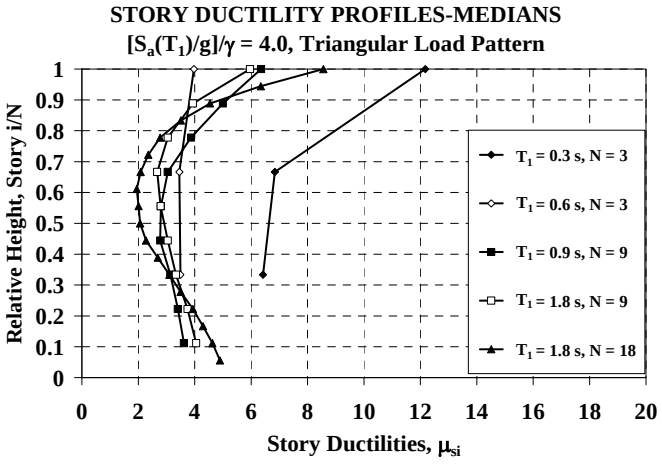

(b)

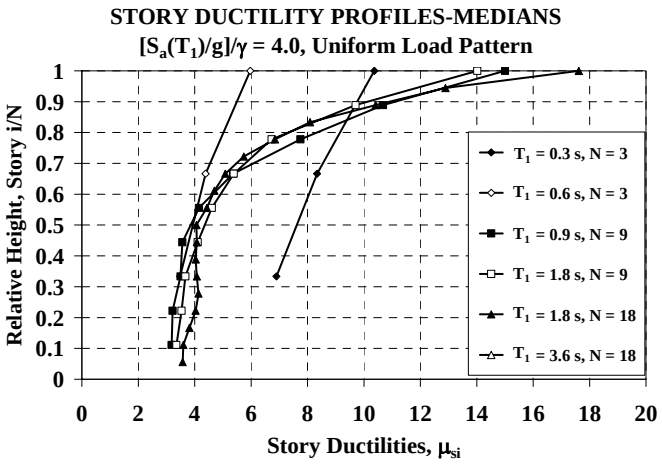

(c)

Fig. 8 Median story ductility profiles, N = 3, 9 and 18, T_1 = 0.1N and 0.2N, $[S_a(T_1)/g]/\gamma$ = 4.0, various design load patterns: (a) parabolic, (b) triangular, and (c) uniform

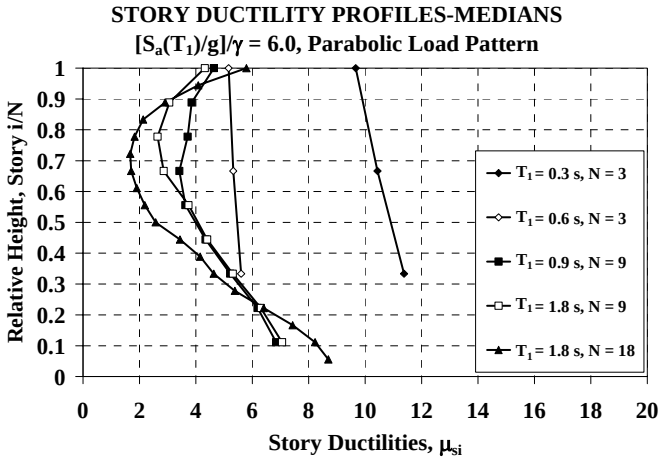

(a)

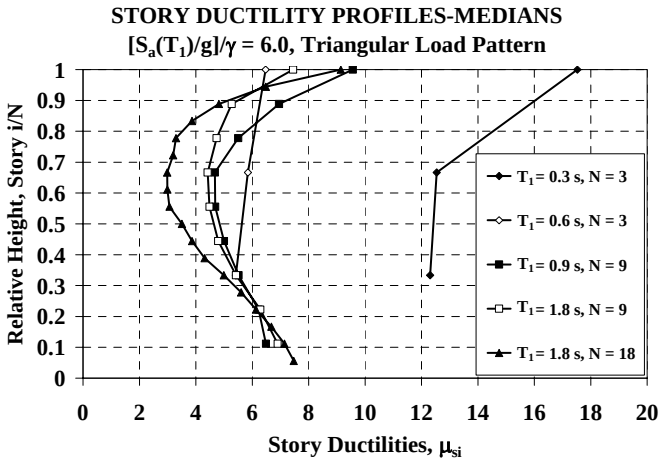

(b)

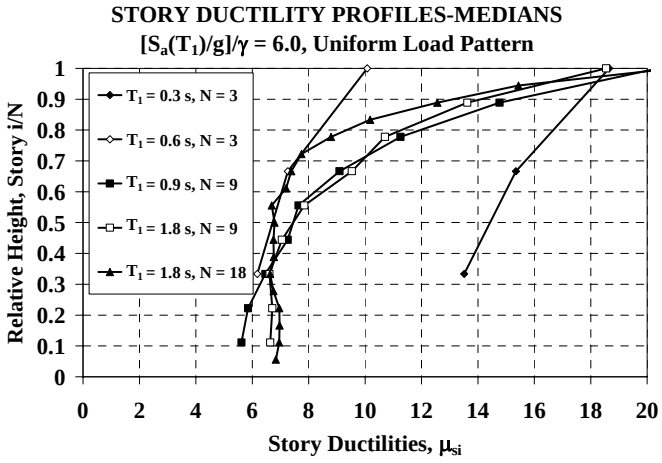

(c)

Fig. 9 Median story ductility profiles, N = 3, 9 and 18, T_1 = 0.1N and 0.2N, $[S_a(T_1)/g]/\gamma$ = 6.0, various design load patterns: (a) parabolic, (b) triangular, and (c) uniform

The information discussed in previous paragraphs has relevant implications for performance-based design. For ordinary ground motions, a different design load pattern is required as a function of the performance target of interest. For instance, if the performance objective is to protect the upper stories from excessive structural damage, under moderate-to-large ground motion intensities, a parabolic load pattern seems to be a logical choice. However, if the objective is to protect the bottom stories from excessive structural damage, a triangular or a uniform load pattern is preferred over a parabolic one.

Furthermore, for structures, that are sensitive to P-Delta effects, the triangular and uniform load patterns are more effective than a parabolic one to limit story deformations, and hence, delay the onset of global instability in the response. At the bottom stories, limiting story drifts is equivalent to limiting story ductilities because for the same strength, the story yield drifts at the bottom of the structures are weakly dependent on the design lateral load pattern.

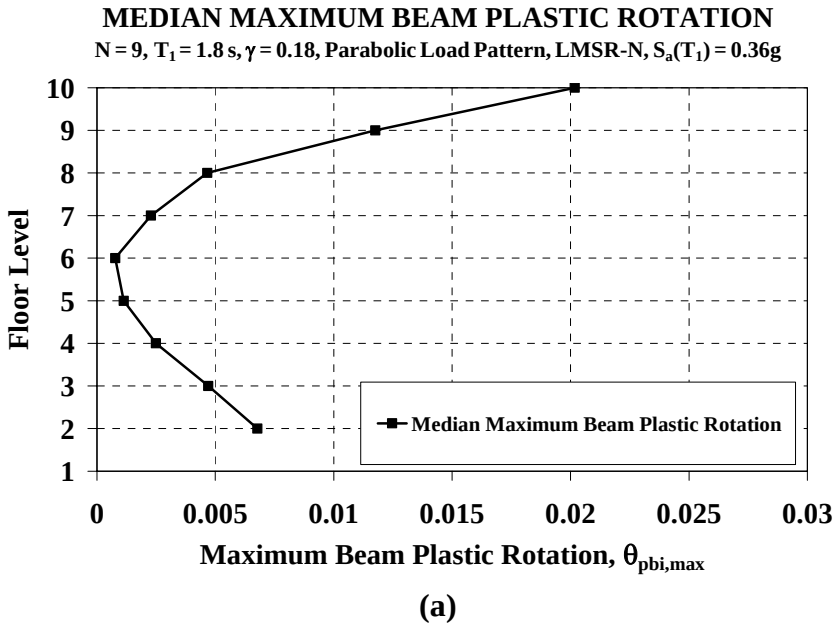

Fig. 10 9-story frame with T_1 = 1.8 s and γ = 0.18 exposed to the LMSR-N ground motion records scaled to S_a(1.8 s) = 0.36g: (a) median maximum beam plastic rotation profile and (b) median maximum story drift angle profile

Given the sensitivity of the distribution of story ductility demands to the design load pattern, a noble objective seems to be to design frames such that a uniform distribution of story ductilities over the height is achieved. Thus, a designer should be able to efficiently utilize the energy capacity available in all structural elements. This topic is the subject of the following section.

STORY SHEAR STRENGTH PATTERNS TO ACHIEVE A UNIFORM DISTRIBUTION OF STRUCTURAL DAMAGE OVER THE HEIGHT

Regular frame structures whose story strengths are tuned to code-compliant lateral load patterns and are exposed to ordinary ground motions exhibit a non-uniform distribution of story ductilities over the height. The basic premise of this study is that story ductilities are an adequate measure of structural damage. Therefore, an important performance target for frames is not only to control the amount of structural damage that is, to limit the story ductilities to a specified value, but also to design structures to have a uniform distribution of structural damage over the height. Achieving this performance target requires extensive knowledge and data on the absolute value and the relative distribution of peak seismic lateral loads. Moreover, controlling the magnitude and distribution of story ductilities over the height has additional benefits for P-Delta sensitive structures for which the onset of global dynamic instability as a function of the relative intensity can be delayed and, in some cases, avoided.

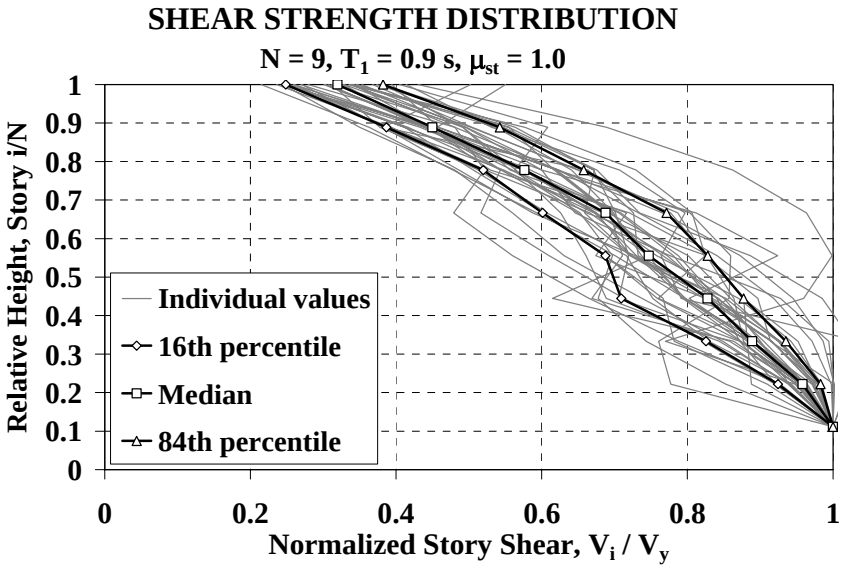

(a)

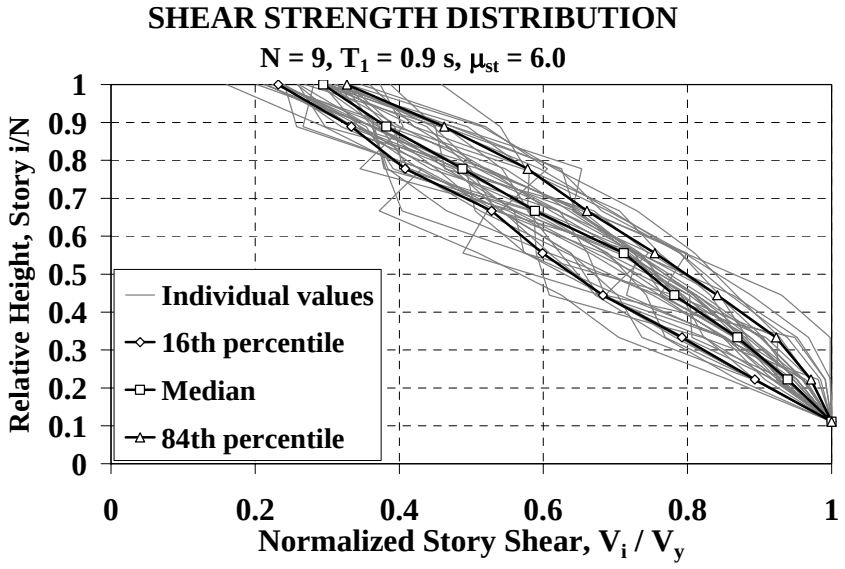

(b)

Fig. 11 Story shear strength patterns to achieve a uniform distribution of story ductilities over the height, $N = 9$, $T_1 = 0.9$ s: (a) $\mu_{st} = 1$ and (b) $\mu_{st} = 6$

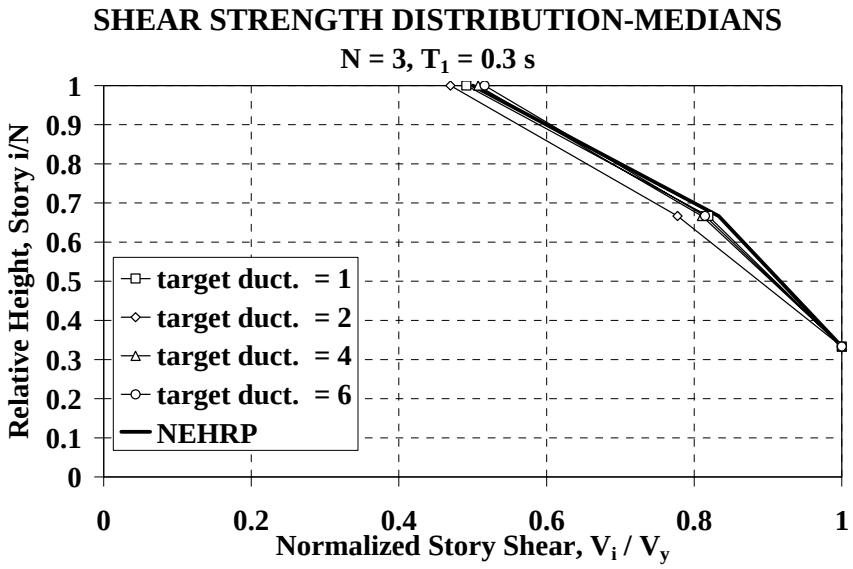

(a)

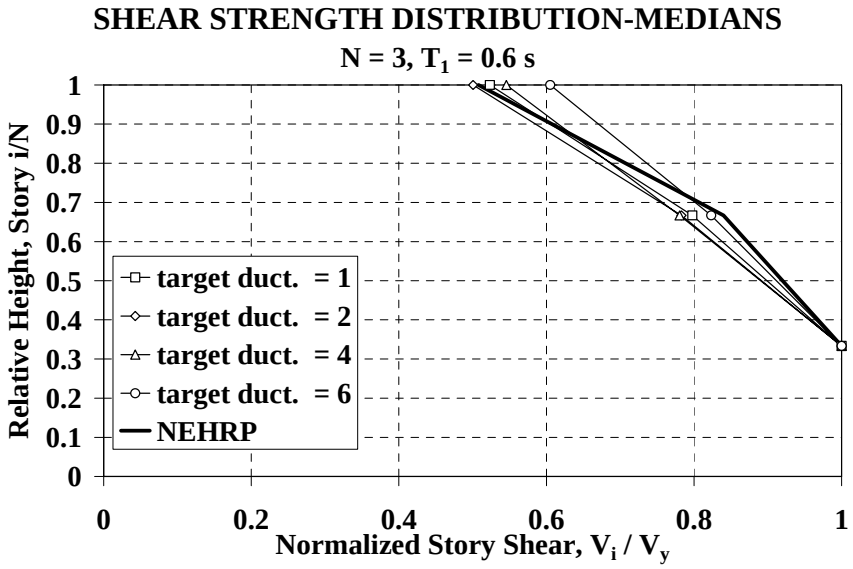

(b)

Fig. 12 Median story shear strength patterns to achieve a uniform distribution of story ductilities over the height, $N = 3$: (a) $T_1 = 0.3$ s and (b) $T_1 = 0.6$ s

An iterative procedure is developed to estimate, for each ground motion and structural model, the relative intensity and the required story shear strength pattern to achieve a uniform distribution of story ductilities over the height. Story ductility is defined as the maximum story drift normalized by the story yield drift obtained from a pushover analysis based on the required lateral load pattern. In this context, story yield drifts are well defined quantities because member strengths are tuned so that simultaneous yielding at all plastic hinge locations occur when the frame is subjected to the required load pattern. Thus, the story yield drift distribution over the height of a frame becomes a function of the choice of lateral load pattern (shear strength distribution) used for design.

This iterative procedure is carried out for the complete family of generic frames subjected to the LMSR-N set of ground motion records. Iterations involve modifying the story shear strength pattern until a target story ductility, μ_{st}, is achieved in all stories. A solution is obtained when, for all stories, the computed story ductility is within 1% of the target story ductility. The target story ductility values of interest, in this study, are 1, 2, 4 and 6. A typical representation of the results obtained from this iterative

procedure is shown in Figure 11 for the $N = 9$, $T_1 = 0.9$ s frame. Note that the dispersion in story shear strength patterns decreases with an increase in the level of inelastic behavior. Larger dispersions for smaller levels of inelastic behavior are associated with a larger relative contribution of higher modes to the response. Moreover, the shape of the distribution of story shear strengths over the height is strongly dependent on the level of inelastic behavior (i.e., target story ductility). Similar conclusions were obtained by Alavi and Krawinkler (2001) when studying the effect of simplified pulses on the response of regular frames. These observations are consistent with those obtained from the rest of the frames analyzed in this study.

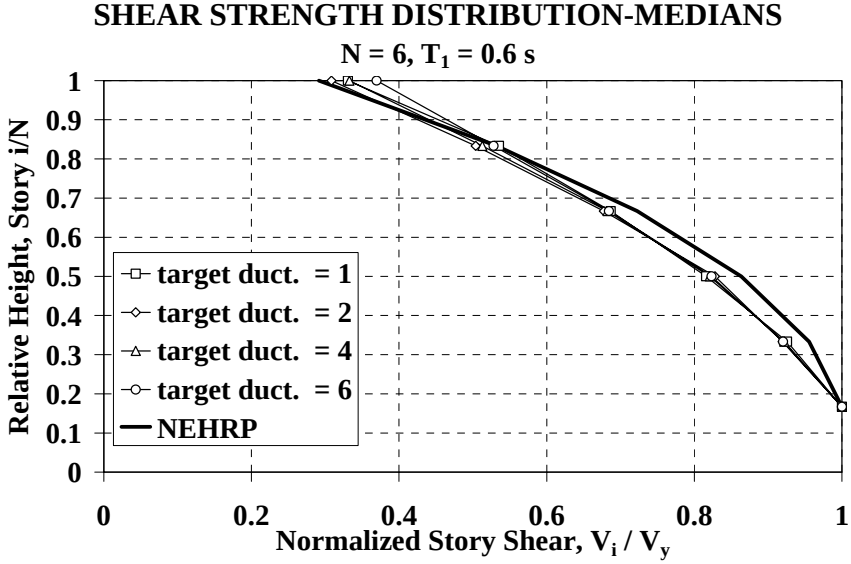

(a)

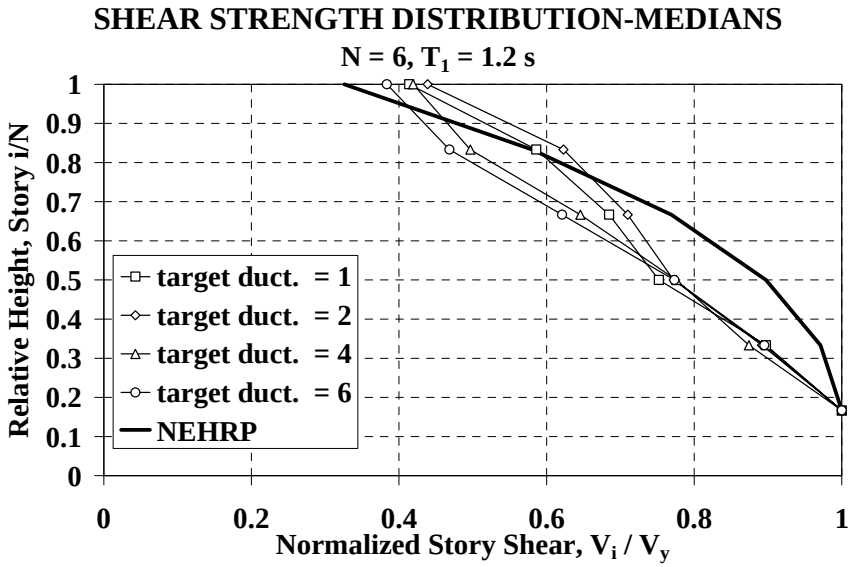

(b)

Fig. 13 Median story shear strength patterns to achieve a uniform distribution of story ductilities over the height, $N = 6$: (a) $T_1 = 0.6$ s and (b) $T_1 = 1.2$ s

Figures 12 to 17 present comprehensive information on median story shear strength patterns as a function of the target story ductility for all frames. The design load pattern based on the NEHRP (FEMA, 2000a) provisions (Equation (1)) is plotted in all graphs for comparison. The NEHRP provisions recommend values of $k = 1$ for structures with periods smaller than 0.5 s and $k = 2$ for periods larger than 2.5 s. For structures with periods between 0.5 s and 2.5 s, k is recommended to be computed by linear interpolation between 1 and 2. In most cases, the median story shear strength patterns required to achieve

a uniform target story ductility distribution differ significantly from the code-compliant story shear strength distribution. For a given structure, there is strong dependence of the median story shear strength distribution on the target story ductility. For example, for small levels of inelastic behavior (μ_{st} = 1.0), the strength of the upper stories relative to the bottom stories is greater than that of the systems with μ_{st} = 6.0. This behavior is attributed to higher mode effects, which predominate in the response of structures that experience relatively small levels of inelastic behavior.

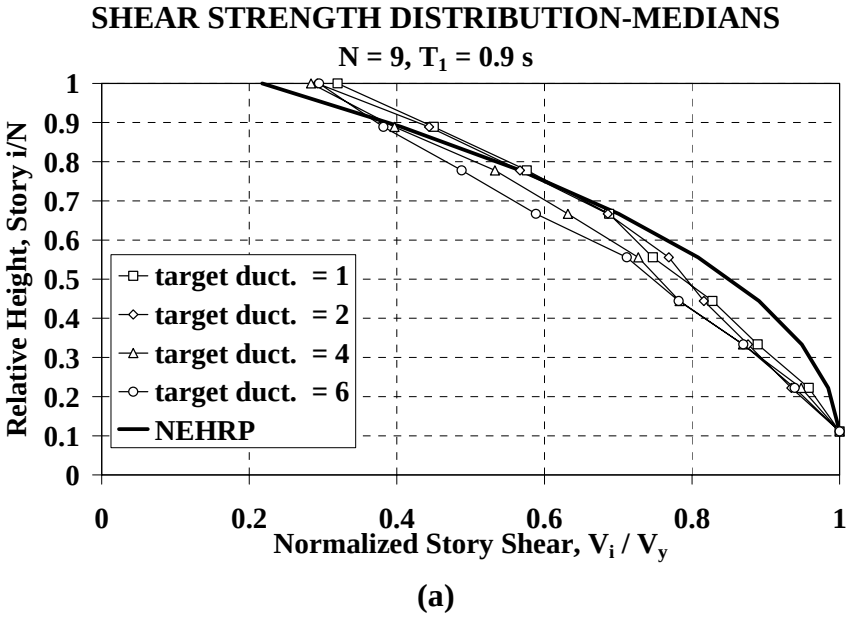

(a)

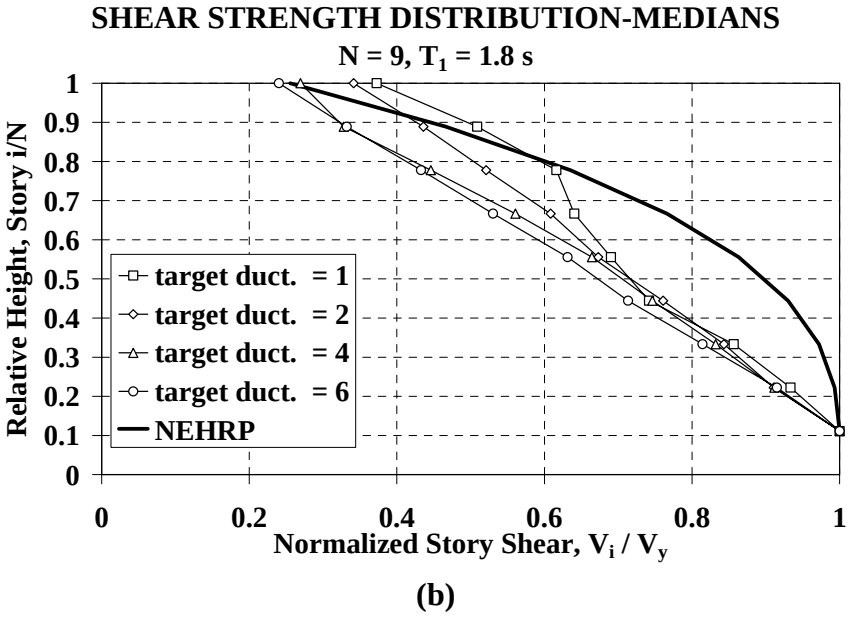

(b)

Fig. 14 Median story shear strength patterns to achieve a uniform distribution of story ductilities over the height, N = 9: (a) T_1 = 0.9 s and (b) T_1 = 1.8 s

Figure 18 depicts the median relative intensities, which together with a tuned design, are needed to achieve a uniform distribution of story ductilities over the height. For cases in which there are overlapping periods (i.e., T_1 = 0.6 s, 1.2 s, and 1.8 s), the required relative intensity to achieve a uniform distribution of story ductilities is weakly dependent on the number of stories. Therefore, the fundamental period is the controlling parameter in this case. The median relative intensities, shown in Figure 18, are rather stable with respect to the fundamental period and in most cases close to the target story ductility, except for (a) short period systems for which smaller relative intensities are required to achieve the same target story ductilities, and (b) tall, flexible frames, especially those sensitive to P-Delta effects. For short-

to-moderate periods and small-to-medium levels of inelastic behavior, the shape of these curves is consistent with the shape of the R-μ_{SDOF}-T curves obtained for SDOF systems (Nassar and Krawinkler, 1991; Miranda and Bertero, 1994; Vidic et al., 1994).

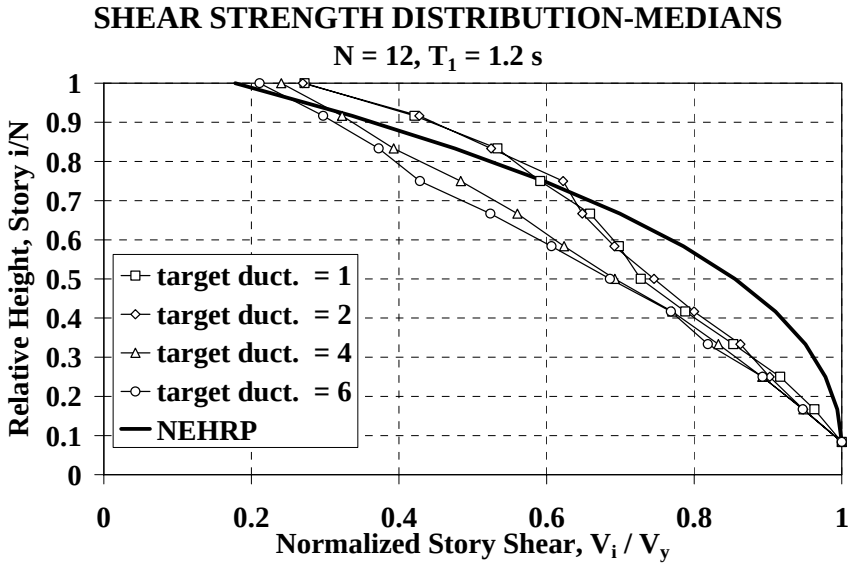

(a)

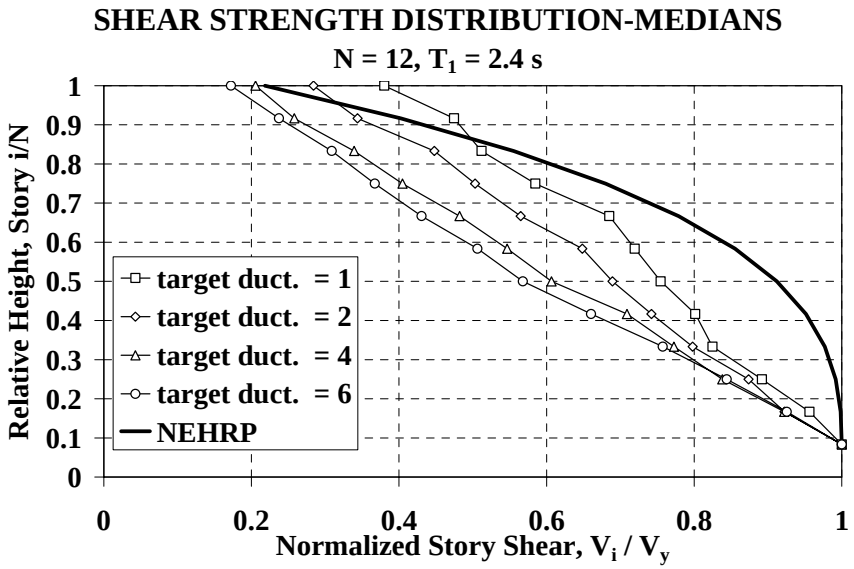

(b)

Fig. 15 Median story shear strength patterns to achieve a uniform distribution of story ductilities over the height, $N = 12$: (a) $T_1 = 1.2$ s and (b) $T_1 = 2.4$ s

STORY SHEAR STRENGTH DISTRIBUTION TO ACHIEVE A TARGET STORY DUCTILITY

In order to quantify the absolute and relative story shear strengths required to achieve a uniform distribution of story ductilities over the height, simplified relationships are computed based on the information presented in Figures 12 to 18. These relationships are a function of the fundamental period, number of stories, and target story ductility. Two different issues that need to be considered in the development of these relationships are: (a) the relative intensity to achieve a target story ductility, and (b) the distribution of story shear strengths over the height.

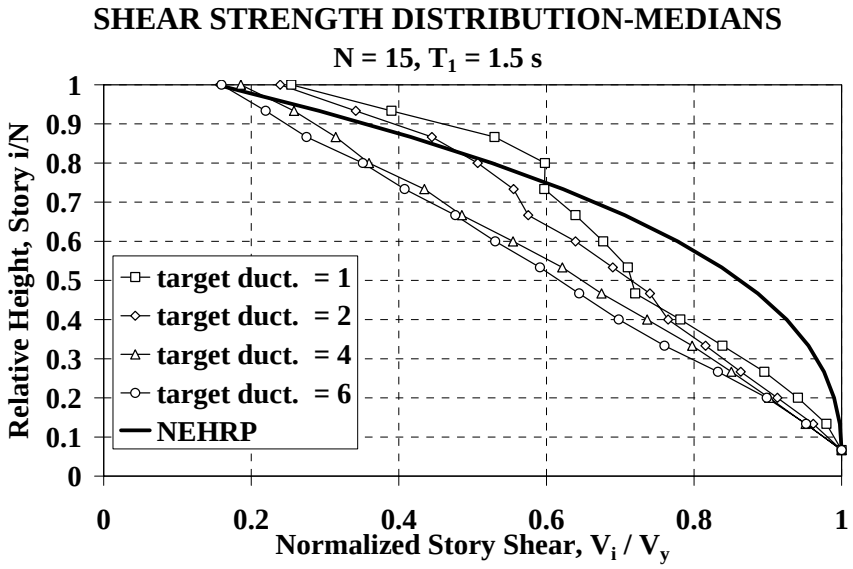

(a)

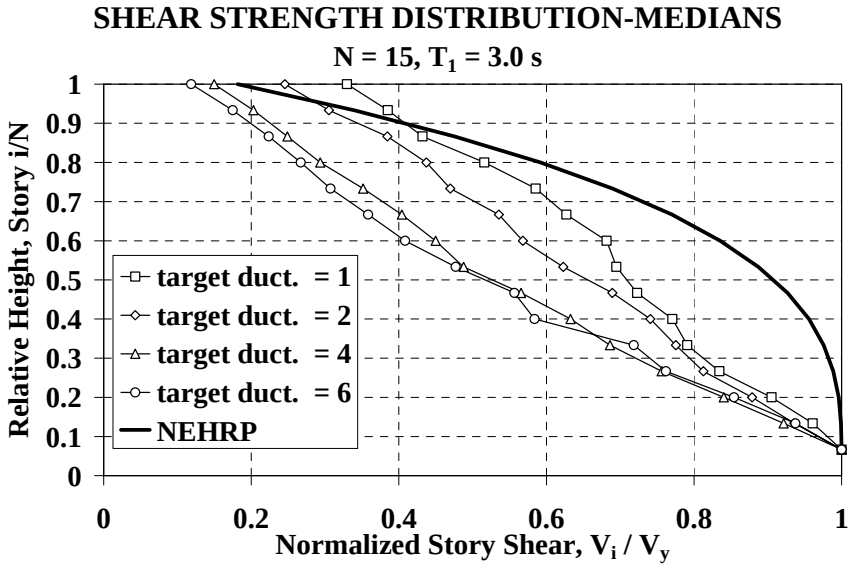

(b)

Fig. 16 Median story shear strength patterns to achieve a uniform distribution of story ductilities over the height, $N = 15$: (a) $T_1 = 1.5$ s and (b) $T_1 = 3.0$ s

1. Relative Intensity to Achieve a Target Story Ductility

R-μ_{SDOF}-T curves, developed by Nassar and Krawinkler (1991) for bilinear SDOF systems exposed to ordinary ground motions, are plotted in Figure 18. Although these R-μ_{SDOF}-T curves are developed for bilinear systems, as it has been previously stated, results obtained by Medina and Krawinkler (2003) demonstrate that the story drift and ductility demands for non-deteriorating, regular frames that exhibit bilinear and peak-oriented hysteretic behavior are very similar. Figure 18 shows that for $\mu_{st} = 2$, 4 and $T_1 \leq 1.8$ s, the relationships developed for SDOF systems can be used to estimate the median relative intensities to achieve a pre-defined target story ductility. For $\mu_{st} = 6$ and $T_1 > 0.6$ s, the required relative intensity decreases approximately inversely proportional to the fundamental period. Moreover, for all target ductilities in Figure 18, the R-μ_{SDOF}-T relationships apply to the short period frame (i.e., $N = 3$, $T_1 = 0.3$ s).

Therefore, within certain limitations, simplified R-μ_{SDOF}-T relationships, developed for SDOF systems and ordinary ground motions, can be used to estimate the median relative intensity to achieve

target story ductilities in the interval $\mu_{st} \leq 4.0$. For $\mu_{st} = 6.0$, the R-μ_{SDOF}-T relationships are applicable in the range $T_1 \leq 0.6$ s. For longer fundamental periods and $\mu_{st} = 6.0$, the median relative intensity decreases inversely proportional to T_1 with an initial value of $[S_a(0.6 \text{ s})/g]/\gamma = \mu_{st}$ and a value of $[S_a(3.6 \text{ s})/g]/\gamma$ approximately equal to $\mu_{st} - 2.5$.

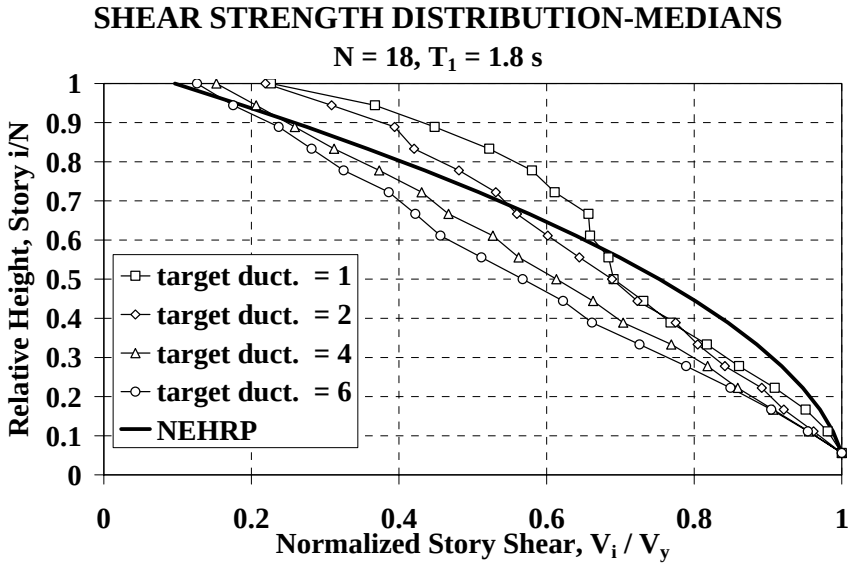

(a)

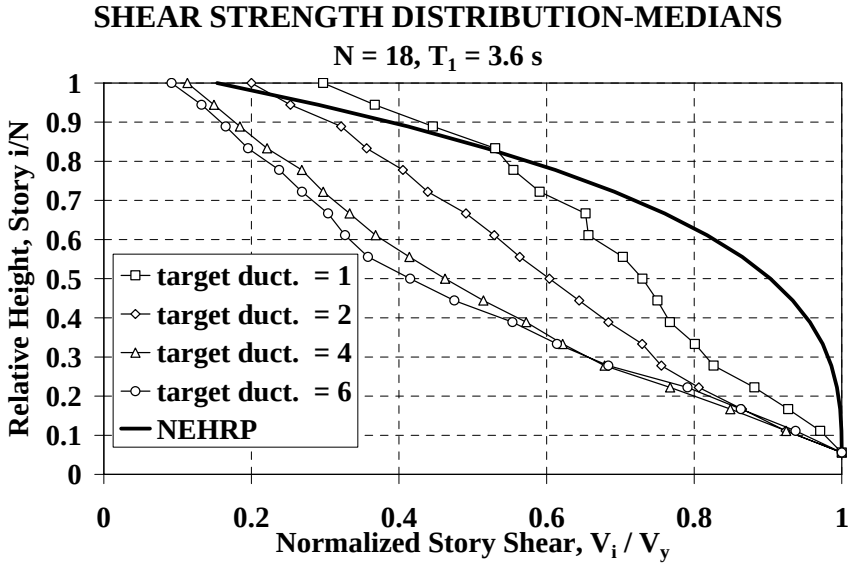

(b)

Fig. 17 Median story shear strength patterns to achieve a uniform distribution of story ductilities over the height, $N = 18$: (a) $T_1 = 1.8$ s and (b) $T_1 = 3.6$ s

2. Distribution of Story Shear Strength over the Height

The information presented in Figures 12 to 17 is analyzed in order to determine the design lateral load pattern to obtain the same target story ductility at all levels. The main assumption is that the seismic lateral load pattern is of the form:

$$F_{x/H} = \begin{cases} F'_{\text{top}} \left(\frac{x}{H}\right)^k & , \quad 0 \le \left(\frac{x}{H}\right) < 1 \\ F_{\text{top}} + F'_{\text{top}} & , \quad \left(\frac{x}{H}\right) = 1 \end{cases} \tag{3}$$

where $F_{x/H}$ is the lateral load at level (x/H), H is the total height of the frame, k is an exponent related to the structure period and the target story ductility, F'_{top} is the lateral load at (x/H) = 1.0 based on the distribution over the height of a total shear equal to ($V_y - F_{\text{top}}$) as a function of k, and $F_{\text{top}} = F_{(x/H\,=\,1)} - F'_{\text{top}}$.

Equation (3) leads to lateral forces along the height of the structure as shown in Figure 19. An expression for the normalized static story shear strength, based on Equation (3), is given by:

$$\frac{V_{x/H}}{V_{x/H=0}} = \left(1 - \frac{F_{\text{top}}}{V_{x/H=0}}\right) \frac{\sum_{z=H}^{x} \left(\frac{z}{H}\right)^k}{\sum_{z=H}^{0} \left(\frac{z}{H}\right)^k} + \frac{F_{\text{top}}}{V_{x/H=0}} \tag{4}$$

where $V_{x/H}/V_{x/H\,=\,0}$ is the story shear at level (x/H) normalized by the story shear at the base ($V_{x/H\,=\,0} = V_y$).

Equation (4) with $F_{\text{top}} = 0$ is equivalent to the normalized story shear strength patterns obtained using Equation (2) when frames have a uniform mass.

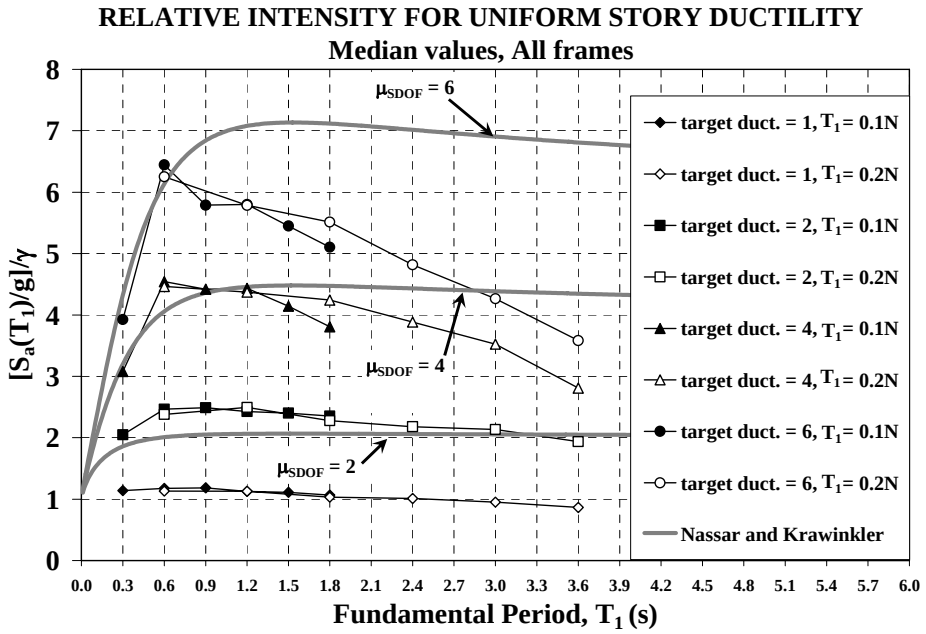

Fig. 18 Median relative intensities, which together with a tuned design, are needed to achieve a uniform distribution of story ductilities over the height, all frames, μ_{st} = 1, 2, 4 and 6

For each structure and target story ductility, an iterative procedure is developed to find the values of k and F_{top} that minimize the error between the median story shear strength patterns, shown in Figure 12 to 17, and the values computed based on Equation (4) (see Figure 20). Although the general shapes of the 16th and 84th percentile results differ from the shape of the median results (Figure 11), median values are used to represent the central tendencies of the results. The error is computed by:

- calculating, for each story, the square of the difference between the median normalized story shear strength pattern and the normalized story shear strength pattern based on Equation (4), and
- adding the square of the differences over the height of the frame to estimate a total error for a given value of k and F_{top}.

Tables 2 to 7 present a summary of the values of k and F_{top}/V_y, obtained from the aforementioned procedure.

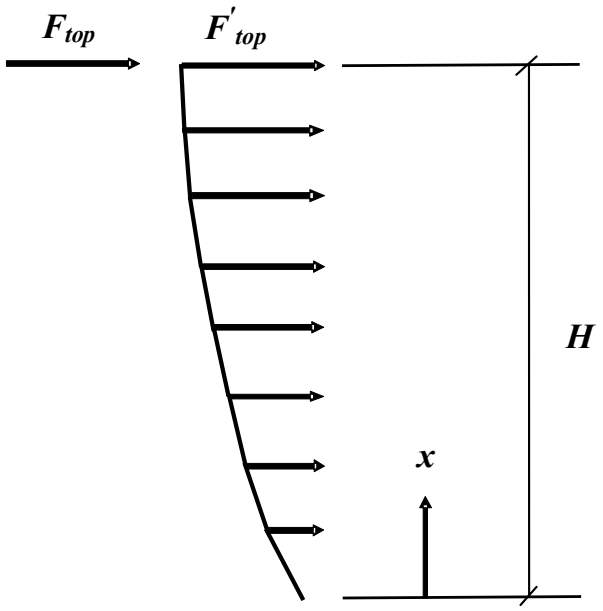

Fig. 19 Proposed design lateral load pattern

Table 2: Calculated Values of k and F_{top}/V_y, N = 3

Number of Stories, N = 3				
Target Story Ductility, μ_{st}	$T_1 = 0.1N$		$T_1 = 0.2N$	
	k	F_{top}/V_y	k	F_{top}/V_y
1	0.85	0.03	0.42	0.02
2	0.46	0.10	0.38	0.17
4	0.67	0.11	0.10	0.30
6	0.69	0.12	0.30	0.36

Table 3: Calculated Values of k and F_{top}/V_y, N = 6

Number of Stories, N = 6				
Target Story Ductility, μ_{st}	$T_1 = 0.1N$		$T_1 = 0.2N$	
	k	F_{top}/V_y	k	F_{top}/V_y
1	0.60	0.13	0.06	0.32
2	0.63	0.09	0.11	0.35
4	0.57	0.13	-0.02	0.29
6	0.50	0.18	0.08	0.23

Table 4: Calculated Values of k and F_{top}/V_y, N = 9

Number of Stories, N = 9				
Target Story Ductility, μ_{st}	$T_1 = 0.1N$		$T_1 = 0.2N$	
	k	F_{top}/V_y	k	F_{top}/V_y
1	0.57	0.20	0.00	0.34
2	0.58	0.18	0.02	0.27
4	0.39	0.17	0.12	0.15
6	0.28	0.17	0.03	0.14

Table 5: Calculated Values of k and F_{top}/V_y, N = 12

Number of Stories, N = 12				
Target Story Ductility, μ_{st}	$T_1 = 0.1N$		$T_1 = 0.2N$	
	k	F_{top}/V_y	k	F_{top}/V_y
1	0.35	0.25	0.16	0.34
2	0.38	0.25	0.04	0.23
4	0.20	0.16	-0.06	0.13
6	0.19	0.12	-0.13	0.10

Table 6: Calculated Values of k and F_{top}/V_y, N = 15

Number of Stories, N = 15				
Target Story Ductility, μ_{st}	$T_1 = 0.1N$		$T_1 = 0.2N$	
	k	F_{top}/V_y	k	F_{top}/V_y
1	0.27	0.29	0.05	0.31
2	0.21	0.23	-0.05	0.22
4	0.11	0.12	-0.25	0.10
6	0.03	0.10	-0.23	0.06

Table 7: Calculated Values of k and F_{top}/V_y, N = 18

Number of Stories, N = 18				
Target Story Ductility, μ_{st}	$T_1 = 0.1N$		$T_1 = 0.2$N	
	k	F_{top}/V_y	k	F_{top}/V_y
1	0.22	0.29	0.12	0.32
2	0.15	0.22	-0.19	0.20
4	0.05	0.11	-0.36	0.07
6	-0.06	0.08	-0.36	0.03

NOTE: k and F_{top}/V_y values for systems with different number of stories, periods and target story ductilities can be estimated by performing linear interpolations of the values shown in Tables 2 to 7.

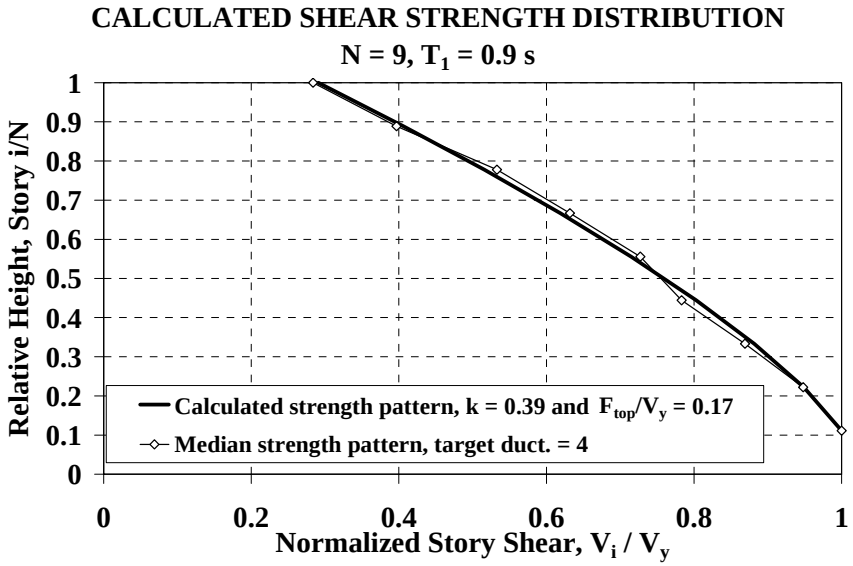

Fig. 20 Calculated shear strength distribution for N = 9, T_1 = 0.9 s, μ_{st} = 4.0

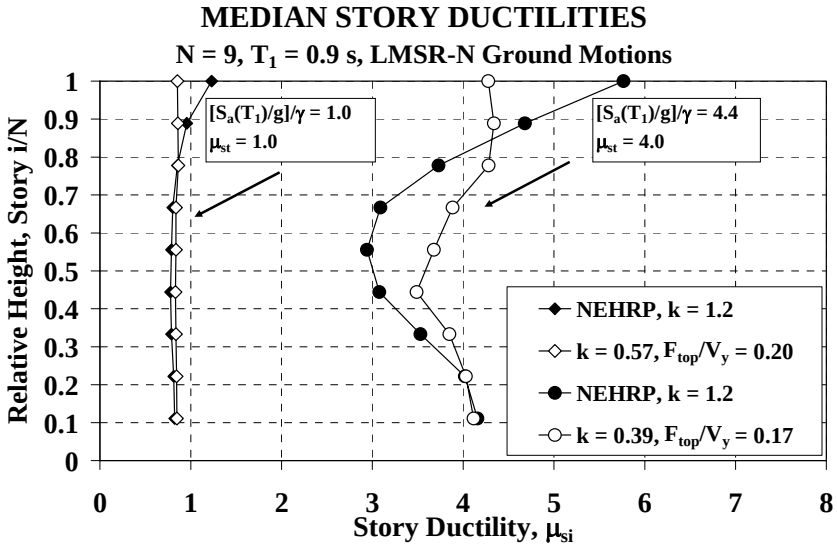

(a)

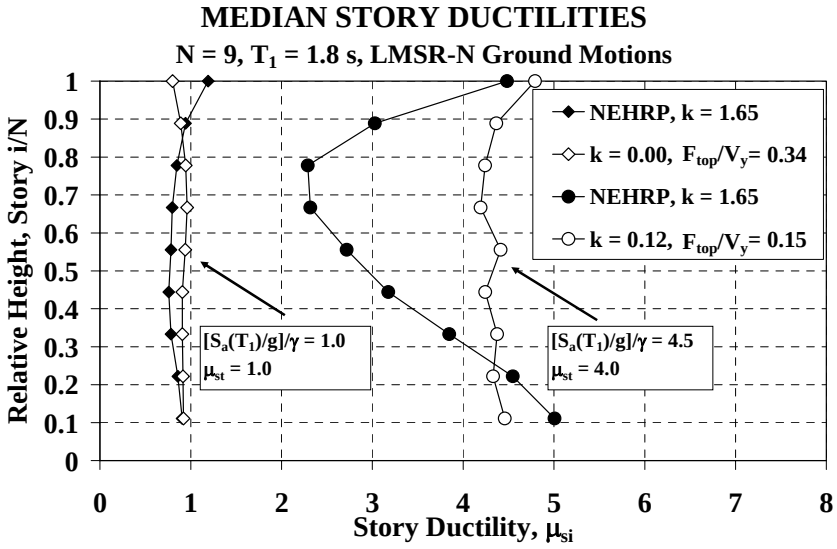

(b)

Fig. 21 Median story ductility profiles of generic frames with $N = 9$, (a) $T_1 = 0.9$ s and (b) $T_1 = 1.8$ s, subjected to the LMSR-N set of ordinary ground motions (NEHRP and proposed design lateral load pattern)

EVALUATION OF ESTIMATED STORY SHEAR STRENGTH PATTERNS

An evaluation is carried out to assess whether the absolute and relative story strength values, estimated in the previous section, are effective to achieve a target story ductility in regular frames subjected to ordinary ground motions. For this purpose, the $N = 9$ frames ($T_1 = 0.9$ s and 1.8 s) are designed based on the proposed load patterns and exposed to the 40 ordinary ground motion records that form the LMSR-N set. In this evaluation, the target story ductility values are equal to 1 (limit of elastic behavior) and 4 (inelastic behavior).

Based on the information presented in Figure 18 and Table 4,

- For $T_1 = 0.1N = 0.9$ s; $\mu_{st} = 1$ and 4,
  - $[S_a(T_1)/g]/\gamma = 1.0$ and 4.4, $k = 0.57$ and 0.39, $F_{top}/V_y = 0.20$ and 0.17
- For $T_1 = 0.2N = 1.8$ s; $\mu_{st} = 1$ and 4,
  - $[S_a(T_1)/g]/\gamma = 1.0$ and 4.5, $k = 0.00$ and 0.12, $F_{top}/V_y = 0.34$ and 0.15

In the median, the distribution of story ductilities over the height of frames that are designed based on the story shear strength distributions proposed in this study is more uniform than that of frames designed based on the NEHRP recommended distributions as it is demonstrated in Figure 21. For a given relative intensity, the proposed story shear strength patterns do not always results in less global structural damage when compared to code-compliant designs (μ_{st} = 4 results in Figure 21(b)). However, results based on the proposed load pattern are consistent with the performance objective of interest, which is to obtain story ductilities approximately equal to four and provide a uniform distribution of damage over the height. Moreover, since both structures have the same base shear strength, but a different shear strength distribution, the structure designed based on the proposed lateral load pattern requires smaller member strengths along its height. Thus, the proposed design load pattern could result in potential cost savings in the design of the frames when compared to a design based on the NEHRP recommended lateral load pattern.

Median maximum story drift angle profiles for the μ_{st} = 4 cases in Figure 21(b) are presented in Figure 22 along with their corresponding story yield drift profiles. The 9-story frame with a base shear coefficient, γ, equal to 0.08 is used for illustration. Differences in the total amount of structural damage, identified in the previous paragraph for Figure 21(b), are mostly attributed to differences in the distribution of story yield drifts over the height (Figure 22).

Results presented in Figure 22 also indicate that although the proposed design load patterns generate designs that in the median produce a rather uniform distribution of story ductility along the height, the distribution of story drift angles remains highly non-uniform. This issue requires special attention particularly within a performance-based design context. If the target performance objective is to limit and distribute the amount of structural damage over the height, designs that give rise to an approximate constant story ductility distribution over the height become relevant (assuming that story ductility is an appropriate structural damage indicator). However, if the story drift angle is considered a more reliable structural damage indicator and/or the target performance objective is to limit nonstructural damage, design load patterns that target a uniform distribution of story drift angles over the height become relevant. Results from this study suggest that, on average, it is unlikely that a uniform distribution of story ductilities and story drift angles over the height will be obtained with the same design load pattern. These issues are the subject of current research efforts carried out by the author at the time of publication of this paper.

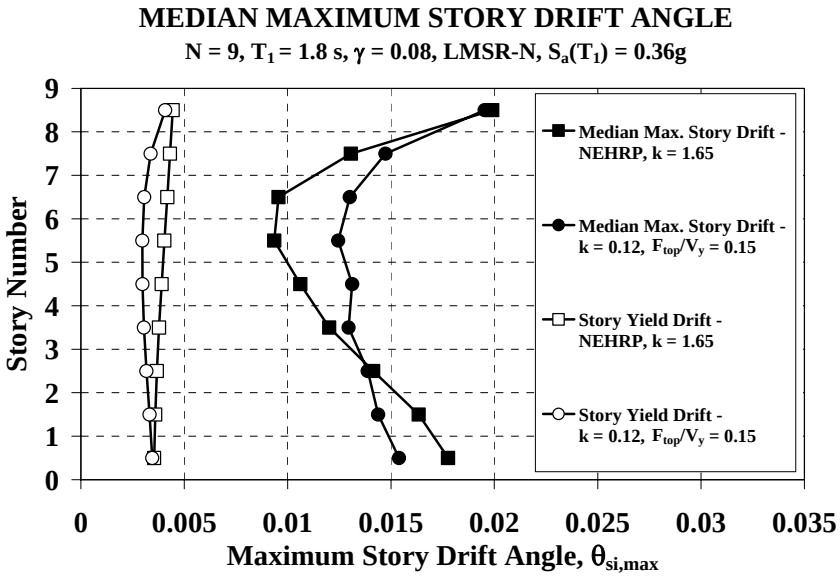

Fig. 22 Median story drift angle profiles and story yield drift profiles for N = 9, T_1 = 1.8 s frame with γ = 0.08 subjected to the LMSR-N ground motion records scaled to S_a(1.8 s) = 0.36g (NEHRP and proposed design lateral load pattern)

SUMMARY AND CONCLUSIONS

This paper discusses the sensitivity of story ductility demands to the design story shear strength pattern for non-deteriorating, regular frames subjected to ordinary ground motions. In this context, the term ordinary refers to ground motions that do not have (a) near-fault, forward directivity; (b) soft soil or (c) long duration characteristics. The regular frames utilized have stiffness degradation at the component level, but do not incorporate cyclic deterioration. Thus, the deformation levels of primary interest are those for which significant cyclic deterioration is not expected to occur ($\mu_{st} \leq 6.0$). For tall, flexible frames, second order, P-Delta effects are considered. All frames are designed such that when they are subjected to the design lateral load pattern, simultaneous yielding occurs at the beam ends and at the bottom of the first story columns. Issues such as the variation of the distribution of stiffness over the height, three dimensional effects, overstrength, the effect of gravity load moments on the beam design, and the contribution of secondary systems are not considered. The conclusions obtained in this study are to be interpreted within these limitations.

It is assumed that the story ductility (defined as the maximum story drift from time history analyses normalized by the story yield drift from the pushover analysis) is an adequate engineering demand parameter to quantify structural damage. Results demonstrate that the distribution of structural damage over the height of regular frames is sensitive to design story shear strength patterns. There is no unique design load pattern to limit the amount of damage at various performance levels. The choice of the design load patterns depends on the ground motion intensity, the level of inelastic deformation and the structural characteristics of the system. Protection of upper stories from excessive structural damage requires, in general, a load pattern that assigns a relatively large portion of the base shear at the upper stories (e.g., the parabolic load pattern). Protection of lower stories from excessive structural damage requires load patterns that distribute the expected base shear demand more evenly along the height of the structure (e.g., the triangular load pattern). Limiting the story ductility demands, and hence, the story drift demands at the bottom stories has beneficial consequences in tall, flexible frames, where the onset of dynamic instability due to P-Delta effects can be delayed and/or prevented.

It is postulated in this study that an ideal design story shear strength distribution would result in a uniform distribution of story ductilities over the height of the frame. Therefore, the designer is able to efficiently utilize the energy capacity available in all structural elements provided that no additional energy dissipation mechanisms are added to the structure (e.g., dampers). A parametric analysis is performed to estimate the required design story shear strength patterns to limit the story ductilities to a target value and achieve a uniform distribution of story ductilities over the height. Results demonstrate that, on average, a design load pattern with an additional load at the top is suitable for this purpose. Given the ground motion characteristics used in this study, the proposed design load patterns are a function of the structural properties and the performance level of interest (i.e., target story ductility). Different target story ductilities are associated with different story shear strength patterns, which is not consistent with current design approaches in which the same story shear strength pattern is used regardless of the performance level of interest.

This work is an important component of performance-based design methods, which target different seismic performance levels as a function of the ground motion input and the structural properties of the system under consideration. Rigorous implementation of performance-based design requires comprehensive and rigorous tools and extensive knowledge and data on ground motions, geological and geotechnical conditions, the soil-foundation-structure system, and the distribution and properties of the nonstructural systems and of building contents. This includes data on randomness/uncertainty of the physical properties describing all these phenomena and subsystems. However, in the meantime, it should be remembered that engineers have to design buildings quickly and efficiently, and their decisions have to be based mostly on well established concepts of strength, stiffness and ductility. For this reason, improving our basic understanding of inelastic dynamic behavior and developing design strength patterns to limit and uniformly distribute the expected damage in a structure are relevant research objectives.

This work provides comprehensive information on static story shear strength patterns that are useful in the conceptual design of frames subjected to ground motion hazards characteristic of ordinary ground motions.

ACKNOWLEDGEMENTS

The author would like to acknowledge the contributions made by four anonymous reviewers of this paper. Their comments and suggestions helped improve its overall quality and are greatly appreciated.

REFERENCES

1. Alavi, B. and Krawinkler, H. (2001). "Effects of Near-Fault Ground Motions on Frame Structures", Report No. 138, John A. Blume Earthquake Engineering Center, Department of Civil and Environmental Engineering, Stanford University, Stanford, CA, U.S.A.
2. ATC (1978). "Tentative Provisions for the Development of Seismic Regulations for Buildings", Report ATC-3 (also NBS Special Publication No. 510), Applied Technology Council, Redwood City, California, U.S.A.
3. ATC (1996). "Seismic Evaluation and Retrofit of Concrete Buildings", Report ATC-40 (also SSC Report No. 96-01, Seismic Safety Commission, State of California, Sacramento, California, U.S.A.), Applied Technology Council, Redwood City, California, U.S.A.
4. FEMA (2000a). "NEHRP Recommended Provisions for Seismic Regulations for New Buildings and Other Structures", Report FEMA-368, Federal Emergency Management Agency, Washington, DC, U.S.A.
5. FEMA (2000b). "Prestandard and Commentary for the Seismic Rehabilitation of Buildings", Report FEMA-356, Federal Emergency Management Agency, Washington, DC, U.S.A.
6. IBC (2003). "International Building Code", International Code Council, Inc., Falls Church, VA, U.S.A.
7. Medina, R.A. and Krawinkler, H. (2003). "Seismic Demands for Nondeteriorating Frame Structures and Their Dependence on Ground Motions", Report No. 144, John A. Blume Earthquake Engineering Center, Department of Civil and Environmental Engineering, Stanford University, Stanford, CA, U.S.A.
8. Miranda, E. and Bertero, V.V. (1994). "Evaluation of Strength Reduction Factors for Earthquake-Resistant Design", Earthquake Spectra, Vol. 10, No. 2, pp. 357-379.
9. Nassar, A.A. and Krawinkler, H. (1991). "Seismic Demands for SDOF and MDOF Systems", Report No. 95, John A. Blume Earthquake Engineering Center, Department of Civil and Environmental Engineering, Stanford University, Stanford, CA, U.S.A.
10. Prakash, V., Powell, G.H. and Campbell, S. (1993). "DRAIN-2DX: Basic Program Description and User Guide", Report UCB/SEMM-93/17, University of California, Berkeley, CA, U.S.A.
11. Vidic, T., Fajfar, P. and Fischinger, M. (1994). "Consistent Inelastic Design Spectra: Strength and Displacement", Earthquake Engineering and Structural Dynamics, Vol. 23, No. 5, pp. 507-521.